Analysis of a Stand-Alone Residential PEMFC Power System with Sodium Borohydride as Hydrogen Source

P.J.R. Pinto[1], V.R. Fernandes[1], A.M.F.R. Pinto[2] and C.M. Rangel[1]

[1]LNEG – Laboratório Nacional de Energia e Geologia, Fuel Cells and Hydrogen Unit,
Paço do Lumiar, 22 1649-038 Lisboa Portugal
[2]CEFT, Departamento de Eng. Química, Universidade do Porto, Faculdade de Engenharia,
Rua Dr. Roberto Frias, 4200-465 Porto, Portugal
email: paulo.pinto@lneg.pt

Abstract

Catalytic hydrolysis of sodium borohydride ($NaBH_4$) has been investigated as a method to generate hydrogen for fuel cell applications. The high purity of the generated hydrogen makes this process an ideal source of hydrogen for polymer electrolyte membrane fuel cells (PEMFCs). In this paper, the possibility of using a $NaBH_4$-based hydrogen generator with a PEMFC for stand-alone residential use is examined. A complete model of the system is developed, based on models taken from literature with appropriate modifications and improvements. Supervisory control strategies are also developed to manage the hydrogen generation and storage and the power flow. The operation and performance of the integrated system over a one-week period under real loading conditions is analyzed through simulation. Finally, results of the analysis are summarized and the limitations/further scope are indicated.

Keywords: *hydrogen generation, sodium borohydride, PEMFC, residential use*

1 Introduction

Fuel cells are an attractive solution for residential self-generation needs because of their high efficiency, low signatures and modularity. Government and industry-led field demonstration programmes of residential fuel cell systems are already being conducted in different countries around the world [1]. Most of the installed systems are based on polymer electrolyte membrane fuel cell (PEMFC) technology and in most of the cases hydrogen is generated in-situ via reforming of fossil fuels such as natural gas or propane [2]. Among the various types of fuel cells, PEMFC appears to be more attractive due to its low operating temperature, higher power density, potential for low cost and volume, fast start-up and suitability for discontinuous operation. Fossil fuels' attraction is that a supply infrastructure already exists and that it is currently the least expensive source of hydrogen.

The most commonly used reforming processes generate poisons or impurities that negatively impact PEMFC performance and durability [3, 4]. Removal of the impurities to yield an acceptably pure hydrogen level renders these methods of hydrogen generation extremely complex and bulky. Other hydrogen generation routes are therefore desired for fuelling PEMFCs.

The hydrolysis of chemical hydrides has been distinguished as a new route of generating hydrogen in-situ for PEMFCs due to the relatively low reaction-initiating temperature and theoretically high hydrogen storage capacity. Among them, sodium borohydride ($NaBH_4$)-based hydrolysis systems has received the most extensive attention owing to their combined advantages of satisfactory reaction controllability, safe fuel storability, and environmentally benign and recyclable reaction by-product. In the presence of a heterogeneous catalyst, a $NaBH_4$ solution with an alkaline stabilizer, NaOH, reacts rapidly with water to generate hydrogen according to the hydrolysis reaction shown in equation (1):

$$NaBH_4 + (2+x)\,H_2O \rightarrow NaBO_2{\cdot}xH2O + 4H_2 + \text{heat} \qquad (1)$$

where x is the hydration factor. Recent progresses in the development of hydrogen generation technology from $NaBH_4$ hydrolysis have been summarized in some reviews [5-7].

PEMFC power systems with $NaBH_4$ as hydrogen source ($NaBH_4$-PEMFC) have been applied and evaluated on portable and vehicular applications by many researchers. The reported results are encouraging although further improvements in both gravimetric and volumetric hydrogen storage capacities are still required with respect to these applications.
For residential applications, the gravimetric and volumetric capacities requirements may not be so stringent. Therefore, the possibility of using a $NaBH_4$-PEMFC system to service the electrical needs of a residential application is here examined.
Starting with synoptic view of the system to be investigated, the dynamic model of each component is formulated. The complete system is then integrated and simulated using Matlab/Simulink®. The main results and insights gained from the simulations are outlined and discussed.

2 System overview

The stand-alone $NaBH_4$-PEMFC power system that is studied in this paper is illustrated in Fig. 1. This system consists of three parts: (1) an in-situ hydrogen generation subsystem, (2) a power generation subsystem and (3) a supervisory control subsystem.

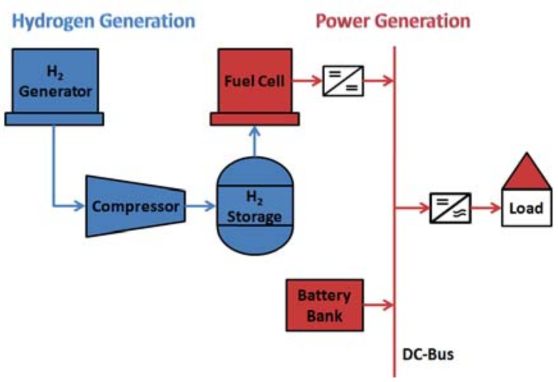

Fig. 1. Layout of the studied stand-alone $NaBH_4$-PEMFC power system.

The hydrogen generation subsystem is considered here to be composed by a batch pressure reactor for hydrogen generation, a pressure tank for hydrogen storage and a compressor for compressing the hydrogen.
The power generation subsystem comprises a PEMFC for hydrogen energy conversion and a battery bank for energy buffering. The low and highly variable load dependent voltage of the PEMFC is boosted to a DC-bus level by a DC-DC converter. The battery bank is directly connected to the DC-bus. The residential load is powered by the DC-AC converter. Using a battery bank together with the PEMFC improves performance and fuel cell lifetime by absorbing faster load changes and preventing fuel starvation of the fuel cell.
The supervisory control subsystem manages the operation of the other subsystems.

3 Model formulation

3.1 Batch pressure reactor

Based on experiments carried out at four different temperatures, a kinetic model has been determined to represent the catalytic hydrolysis of an alkaline $NaBH_4$ in a batch reactor. The experiments were performed in a reaction volume of 369 mL containing 20 mL of 10 wt% $NaBH_4$ solution, including 3 wt% sodium hydroxide (NaOH) solution as an alkaline stabilizer and 1 g of nickel-ruthenium based catalyst at average solution temperatures of 24, 28, 38 and 48 ºC. Some of the specific details of experimental procedures are explained on an earlier work [8].

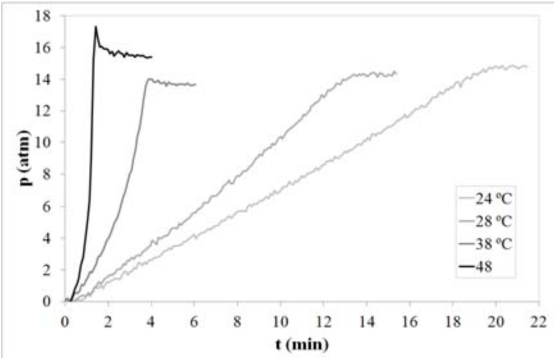

Fig. 2. Hydrogen generation from sodium borohydride hydrolysis on nickel-ruthenium catalyst expressed as the reactor pressure vs. reaction time, for different average temperatures of the working solution.

A zero-order kinetic expression was found to describe the rate of consumption of $NaBH_4$ (c_{NaBH4}).

$$\frac{dc_{NaBH_4}}{dt} = -r_{NaBH_4} = -A\exp\left(\frac{-E_a}{RT_{BR}}\right) \tag{2}$$

where c is the concentration (mol L^{-1}), r the rate of reaction (mol L^{-1} min^{-1}), A the pre-exponential factor (mol L^{-1} min^{-1}), Ea the activation energy for the reaction (kJ mol^{-1}), R the gas constant (kJ mol^{-1} K^{-1}), and T_{BR} is the reaction temperature (K). According to the Arrhenius equation, the plot of $\ln(r_{NaBH4})$ versus $1/T_{BR}$ for four temperature settings as shown in Fig. 3 gave a good linear regression with the correlation coefficient of 0.9971. The activation energy and the pre-exponential factor can then be obtained from the slope and intercept of the regression line, being 75.3 kJ mol^{-1} and 2.41 x 10^{12} mol L^{-1} min^{-1}, respectively.

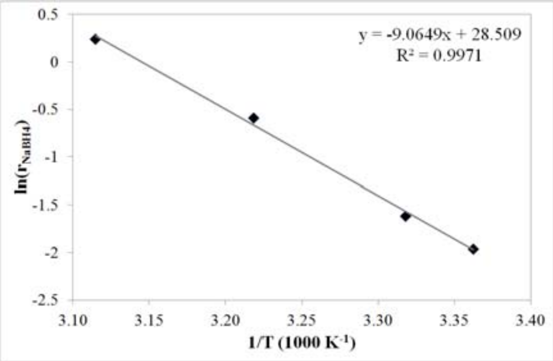

Fig. **3**. Arrhenius plot for the zero-order model for the sodium borohydride hydrolysis on nickel-ruthenium catalyst.

With the kinetic model available, a batch reactor model can be developed. From the mole balance and the stoichiometric relationship the variation of the number of moles of $NaBH_4$, H_2O and $NaBO_2$ with respect to time can be expressed by:

$$\frac{d(vc_{NaBH4})}{dt} = (-r_{NaBH4})v \qquad (3)$$

$$\frac{d(vc_{H2O})}{dt} = 2(-r_{NaBH4})v \qquad (4)$$

$$\frac{d(vc_{NaBO2})}{dt} = r_{NaBH4}v \qquad (5)$$

where v is the solution volume (L) with respect to time, which is evaluated as follows:

$$v = \frac{n_{NaBH4}M_{NaBH4}}{\rho_{NaBH4}} + \frac{n_{H2O}M_{H2O}}{\rho_{H2O}} + \frac{n_{NaBO2}M_{NaBO2}}{\rho_{NaBO2}} \qquad (6)$$

where n is the number of moles (mol), M the molecular weight (g mol^{-1}) and ρ the density (g L^{-1})
The hydrogen pressure buildup in the batch reactor can be computed as follows:

$$p_{BR} = \frac{4(r_{NaBH4}v)\frac{M_{H2}}{\rho_{H2}}}{V_{BR} - v} \qquad (7)$$

where p_{BR} is the hydrogen batch reactor pressure (atm) and V_{BR} the volume of the batch reactor (L). Because of the constant reaction temperature, the energy balance equations are negligible in this system.
In this simulation study, the reaction temperature is assumed constant at 24 ºC. As can be seen in Fig. 4, the zero-order kinetic model describes the experimental data at this temperature reasonably well.

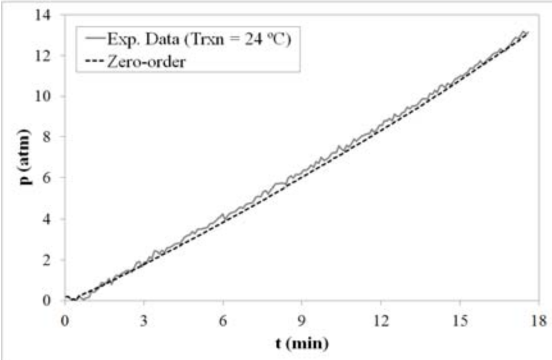

Fig. **4**. Zero-order model prediction with the experimental data at 24 ºC for the sodium borohydride hydrolysis on nickel-ruthenium catalyst.

3.2 Compressor and storage tank

The compressor is modeled assuming ideal gas undergoing a polytropic process. The relationship between the hydrogen molar flow rate dn_{Comp_H2}/dt (mol s^{-1}) and the compressor power P_{Comp} (W) is:

$$\frac{dn_{Comp\_H2}}{dt} = \frac{\alpha_{Comp}}{w} P_{Comp} \qquad (8)$$

and

$$w = \frac{kRT_{BR}}{k-1}\left[\left(\frac{p_{Tank}}{p_{BR}}\right)^{\frac{k-1}{k}} - 1\right] \qquad (9)$$

where w is the polytropic work (J mol^{-1}), α_{Comp} is the compressor efficiency, k is the polytropic coefficient, T_{BR} is the inlet gas temperature (K) (corresponding to the hydrogen temperature in the batch reactor), p_{BR} is the inlet gas pressure (atm) (corresponding to the hydrogen pressure in the batch reactor), p_{Tank} is the outlet gas pressure (atm) (corresponding to the hydrogen pressure in the tank).
The stored hydrogen rate in the tank depends upon the difference between the inflow rate and the outflow rate. Thus, the pressure of stored hydrogen in the tank can be expressed as:

$$\frac{V_{Tank}}{RT_{Tank}}\frac{d}{dt}p_{Tank} = \frac{dn_{Comp\_H2}}{dt} - \frac{dn_{FC\_H2}}{dt} \qquad (10)$$

where T_{Tank} and V_{Tank} are the temperature (K) and the volume (L) of hydrogen inside the tank, respectively, and dn_{FC_H2}/dt is defined in the following section.

3.3 PEMFC

The stored hydrogen is utilized to generate electrical energy based on the load requirement through the PEMFC. The PEMFC power output is managed via the DC-DC boost converter. Here, the boost converter is represented by an ideal power source where the ratio from its output power to its input power is dictated by its efficiency η_{Bo} [10]:

$$P_{Bo} = \eta_{Bo} P_{FC} \Leftrightarrow u_{Bus} i_{FC\_Bus} = \eta_{Bo} u_{FC} i_{FC} \tag{11}$$

where P_{FC}, u_{FC} and i_{FC} are the PEMFC output power (W), voltage (V) and current (A); u_{Bus} is the DC-bus voltage (V) and i_{FC_Bus} is the current from the boost converter to the DC-bus (A). The fuel cell's voltage can be expressed by:

$$u_{FC} = U_{FC\_0} + C_{1\_FC} T_{FC} + C_{2\_FC} \ln\left(\frac{i_{FC}}{I_{FC\_0}}\right) + \frac{R_{FC} i_{FC}}{T_{FC}} \tag{12}$$

where T_{FC} is the PEMFC's operating temperature (ºC); U_{FC_0} (V), C_{1_FC} (V ºC^{-1}), C_{2_FC} (V), R_{FC} (Ω ºC) and I_{FC_0} (A) are constants that were determined experimentally for temperatures ranging from 24 ºC to 72 ºC [11]. Here, the PEMFC's operating temperature is assumed constant at 70 ºC.
Combining equations (11) and (12) yields an expression linking the fuel cell's current to the boost converter's input power which is solved using the Newton-Raphson method. The hydrogen's rate of consumption, $dn_{FC\text{-}H2}/dt$ (mol s^{-1}), by the PEMFC can there be computed using the following expression:

$$\frac{dn_{FC\_H2}}{dt} = \frac{N_{FC} i_{FC}}{\eta_{FC} zF} \tag{13}$$

where N_{FC} is the number of cells, z is the number of moles of electrons for moles of water ($z=2$), F is Faraday's constant (C mol^{-1}) and η_F is the PEMFC Faraday's efficiency that is here assumed constant and equal to 0.9.

3.4 Battery bank

A simplified model of the lead-acid battery bank can be constructed by an ideal constant voltage source, U_{Bat} (V), in series with an equivalent internal resistance, R_{Bat} (Ω), and an equivalent capacitance, C_{Bat} (F) [12]. Knowing the current, i_{Bat_Bus}, voltage is given by:

$$u_{Bat} = U_{Bat} + \left(i_{Bat\_Bus} R_{Bat} + \frac{1}{C_{Bat}} \int i_{Bat\_Bus} dt \right) \eta_{Bat} \tag{14}$$

The battery bank efficiency, η_{Bat}, is considered to be equal to 0.85 during charging and equal to 1 during discharging.

3.5 Load supply

The current supplied to the load must be converted by a DC-AC converter (inverter) with efficiency η_{inv} and is given by:

$$i_{Bus\_Load} = \frac{P_{Load}}{\eta_{Inv} u_{Bus}} \tag{15}$$

where P_{Load} is the load power.

3.6 Supervisory control

To coordinate the overall system, a supervisory control algorithm detects working conditions and decides how to operate each subsystem.
Control of the hydrogen generation subsystem is based on the pressure levels of hydrogen gas in the batch reactor and in the storage tank. A new batch reaction is initiated whenever the pressure of hydrogen gas in the storage tank falls to or is below a predetermined level (p_{BR_Start}, established based on the amount of hydrogen produced in each batch reaction). The compressor is started up whenever the pressure of hydrogen gas in the batch reactor reaches a level indicative of reaction completion (p_{Comp_Start}) and is shut down as soon as the pressure in the batch reactor falls to the atmospheric pressure. A minimum time interval (t_{Min}) is established between the decompression of the batch reactor and the start of a new reaction in order to take into account the time spent on tasks such as removing reaction by-products, feeding a new solution and reaching the desired reaction temperature.
Control of the power generation subsystem is based on the DC-bus Eq. (16) that balances the electrical currents entering (positive sign) or exiting the DC-bus (negative sign):

$$i_{FC\_Bus} - i_{Bus\_Load} \pm i_{Bat\_Bus} = 0 \tag{16}$$

When the load requires more current than the PEMFC can provide at that moment, the battery bank fills this gap by releasing a positive i_{Bat_Bus} (from battery to DC-bus). Otherwise, the PEMFC should recharge the battery bank if necessary (with a negative i_{Bat_Bus}, from DC-bus to battery bank), making sure not to exceed the maximum current that the PEMFC can provide. The current request from the control to the PEMFC should be equal to the current needed by the load plus the current needed to recharge the battery bank. To avoid overvoltage at DC-bus, the current needed to recharge the battery bank is calculated as a function of the battery bank voltage (Eq. 17).

$$i_{Bus\_Bat} = I_{Bat\_Max} \min\left(1, \frac{U_{Bus\_Max} - u_{Bus}}{U_{Bus\_Band}}\right) \quad (17)$$

Where I_{Bat_Max} is the maximum battery charging current (A); U_{Bus_Max} is the defined maximum DC-bus voltage (V) and U_{Bus_Band} is the defined voltage band (V).

4 Simulation and results

The dynamic models of the $NaBH_4$-PEMFC system, as discussed in the preceding sections, are implemented in Matlab/Simulink® environment to get an overview of system's behavior over a long period of time. To achieve this, the system is simulated for a complete week using an integration step of 30s. While this value is high, it has no significant impact on the precision of the results because there is no fast dynamics in the model.

The $NaBH_4$-PEMFC system (Fig. 1) is sized to supply power to a 3-person (1 adult and 2 children) dwelling. The purpose of the study is to properly size the system components to assure reliable electricity supply. Hence, the system's economic aspect is not considered in the paper.

The load profile is taken from Ref. [12] and it represents a standard European domestic electrical energy consumption. One-week period data, acquired during November and averaged over a 5 minute time interval, comprises the data set for the analyses presented herein. The average and peak load demand is 0.52 kW and 5.21 kW, respectively. Here, a 5kW PEMFC is assumed for the system. The battery bank should be capable of providing the peaking load in surplus of what can be met by the fuel cell and the transient peaks of load. The selected profile has slow load changes, which can be followed by the PEMFC. Therefore, a 2 kWh battery bank is sufficient for this study. The pressurized tank is sized to store the amount of hydrogen needed by the PEMFC to supply the daily average load energy. Hydrogen holds 3 kWh of energy per cubic meter (lower heating value) and the daily average load energy is 12.4 kWh. Assuming that the efficiencies of the PEMFC and power converters are 40% and 90%, respectively, the volume of hydrogen needed by the PEMFC is determined to be 12815 L. To store this amount of hydrogen in pressure tank pressurized at 100 atm, a pressure tank with an approximate volume of 128 L is required. The batch pressure reactor model developed in Section 3.1 is scaled-up by a factor of 250 to generate approximately 1180 L of hydrogen, which is a little more than the amount of hydrogen needed by the PEMFC to supply the two-hourly average load energy. The values of the system parameters used in the simulation study are given in the Appendix.

From our simulation runs, the designed system has a successful performance at meeting the requirements.

Fig. 5 provides the insight into currents' dynamics on the DC-bus, showing how the load current is shared among the PEMFC and the battery bank. As expected, the battery bank absorbed the peaking load in surplus of what could be met by the PEMFC. Moreover, after each discharge of the battery bank, the PEMFC was able to recharge it again.

Fig. 6 shows the pressures dynamics of the batch reactor and the storage tank. It can be seen that whenever the hydrogen storage tank pressure crosses the threshold p_{BR_Start} and a minimum time interval, t_{Min}, has elapsed after the decompression of the batch reactor, a new reaction is initiated. It can also be seen that the hydrogen storage tank pressure is maintained at a reasonable level.

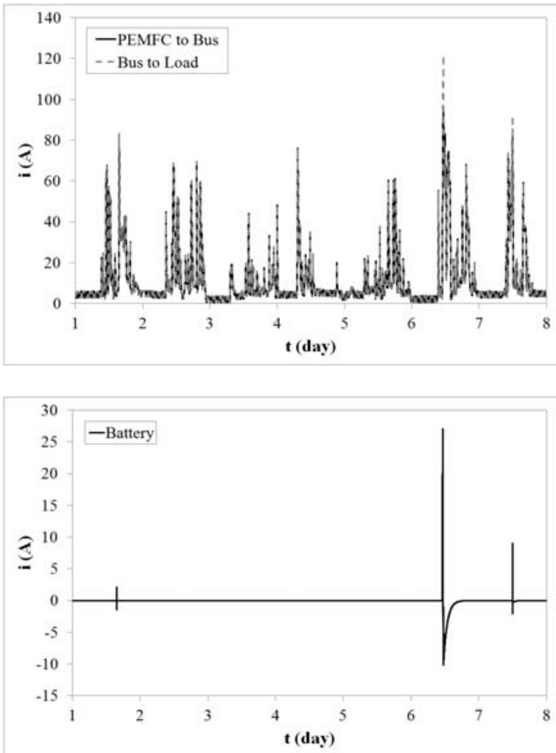

Fig. 5. Dynamics of currents at the DC-bus.

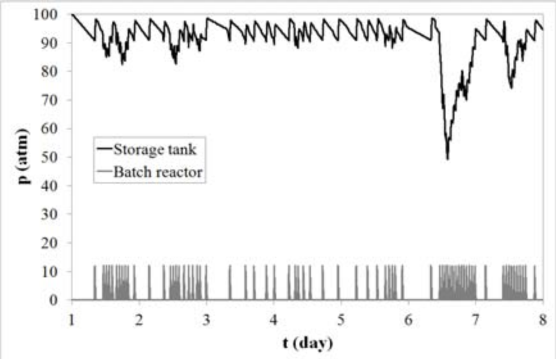

Fig. 6. Dynamics of pressure of hydrogen gas in the batch reactor and in the storage tank.

5 Conclusion

The performance of a residential scale $NaBH_4$-PEMFC stand-alone power system over a one-week period under real loading conditions is analyzed by numerical simulation. The results show that the variables under interest are regulated while fulfilling the operating requirements, thereby proving the effectiveness of the overall supervisory control strategy and the feasibility of the $NaBH_4$ hydrolysis reaction as the hydrogen supplying method for the PEMFC system. Major limitation, however, to implement the scheme in real system is the $NaBH_4$ cost.

With more research in this field, it can be expected that the economics would be favorable in the future with advancements for example in the recycling of reaction by-products back to borohydride. Likewise, model validation with the real/experimental situation is expected for further insights of the scheme.

References

[1] Breakthrough Technologies Institute, Inc. 2010 Fuel Cell Technologies Market Report. In: Program USDFCT, editor. Washington (DC): US DOE EERE fuel cell technologies program; 2011. <http://www1.eere.energy.gov/hydrogenandfuelcells/pdfs/2010_market_report.pdf>.

[2] K-A. Adamson. 2009 Fuel Cell Today - Small Stationary Summary Report. Fuel Cell Today 2009. <http://www.fuelcelltoday.com/media/pdf/surveys/2009-Small-Stationary-Free-Report-2.pdf>.

[3] R. Borup, J. Meyers, B. Pivovar, Y.S. Kim, R. Mukundan, N. Garland, et al. Scientific aspects of polymer electrolyte fuel cell durability and degradation. *Chemical Reviews* 107 (2007) 3904-51.

[4] W. Schmittinger and A. Vahidi. A review of the main parameters influencing long-term performance and durability of PEM fuel cells. *J. Power Sources* 180 (2008) 1-14.

[5] B.H. Liu and Z.P. Li. A review: hydrogen generation from borohydride hydrolysis reaction. *J. Power Sources* 187 (2009) 527-34.

[6] S.S. Muir and X. Yao. Progress in sodium borohydride as a hydrogen storage material: development of hydrolysis catalysts and reaction systems *Int. J. Hydrogen Energy* 36 (2011) 5983-97.

[7] R. Retnammaa, A.Q. Novais and C.M. Rangel. Kinetics of hydrolysis of sodium borohydride for hydrogen production in fuel cell applications: A review. *Int. J. Hydrogen Energy* 36 (2011) 9772-90.

[8] A.M.F.R. Pinto, D.S. Falcão, R.A. Silva and C.M. Rangel. Hydrogen generation and storage from hydrolysis of sodium borohydride in batch reactors. *Int. J. Hydrogen Energy* 31 (2006) 1341–7.

[9] S. Kélouwani, K. Agbossou and R. Chahine. Model for energy conversion in renewable energy system with hydrogen storage. *J. Power Sources* 140 (2005) 392-99.

[10] A. Bilodeau and K. Agbossou. Control analysis of renewable energy system with hydrogen storage for residential applications. *J. Power Sources* 162 (2006) 757-64.

[11] B.S. Borowy and Z.M. Salameh. Dynamic response of a stand-alone wind energy conversion system with battery energy storage to a wind gust. *IEEE Trans. on Energy Conversion* 12 (1997) 73 – 78.

[12] IEA/ECBCS Annex 42. European Electrical Standard Profiles. [Data Files] 2006. <http://www.ecbcs.org/docs/Annex_42_European_Electrical_Specifc_Profiles_Annex_42_September_2006.zip>.

Appendix

Table A1. Models' parameters.

Component	Parameter	Value
Batch reactor	A (mol L^{-1} min^{-1})	2.41x10^{12}
	E_a (kJ mol^{-1})	75.3
	t_{Min} (s)	1800
	T_{BR} (ºC)	24
	V_{BR} (L)	92
	v (L) at t = 0 s	5
Battery	C_{Bat} (F)	15000
	$I_{Bat\ Max}$ (A)	30
	R_{Bat} (Ω)	0.264
	U_{Bat} (V)	42
	$U_{Bus\ Max}$ (V)	55.2
	$U_{Bus\ Band}$ (V)	4
Compressor	α_{Comp}	0.70
	k	1.475
	P_{Comp} (W)	500
	$p_{Comp\ Start}$ (atm)	13.2
PEMFC	$C_{1\ FC}$ (V ºC^{-1})	-0.013
	$C_{2\ FC}$ (V)	-1.57
	$I_{FC\ 0}$ (A)	8.798
	N_{FC}	35
	R_{FC} (Ω ºC^{-1})	-2.04
	$U_{FC\ 0}$ (V)	33.18
	T_{FC} (ºC)	70
	η_{Bo}	0.90
Hydrogen storage	$p_{BR\ Start}$ (atm)	91
	$p_{Tank\ Max}$ (atm)	100
	T_{Tank} (ºC)	25
	V_{Tank} (L)	128